Numerical simulation of the effect of dissipation and phase fluctuation in a direct communication scheme

2015 J. Phys. B: At. Mol. Opt. Phys. 48 115506

(http://iopscience.iop.org/0953-4075/48/11/115506)

IOP Publishing Journal of Physics B: Atomic, Molecular and Optical Physics
J. Phys. B: At. Mol. Opt. Phys. **48** (2015) 115506 (11pp) doi:10.1088/0953-4075/48/11/115506

Numerical simulation of the effect of dissipation and phase fluctuation in a direct communication scheme

Fu Li[1], Jun-Xiang Zhang[2] and Shi-Yao Zhu[1,3]

[1] Beijing Computational Science Research Center, Beijing 100084, People's Republic of China
[2] The State Key Laboratory of Quantum Optics and Quantum Optics Devices, Institute of Opto-Electronics, Shanxi University, Taiyuan 030006, People's Republic of China
[3] Hefei National Laboratory for Physical Sciences at Microscale and Department of Modern Physics, University of Science and Technology of China, Hefei, Anhui 230026, People's Republic of China

Received 16 October 2014, revised 18 March 2015
Accepted for publication 24 March 2015
Published 17 April 2015

Abstract

Recently, the direct counterfactual communication protocol, proposed by Salih *et al* (2013 *Phys. Rev. Lett.* **110** 170502) using a single photon source under ideal conditions (no dissipation, no phase fluctuation and an infinite number of beam splitters), has attracted much interest from a broad range of scientists. In order to put the direct communication protocol into a realistic framework, we numerically simulate the effect of the dissipation and the phase fluctuation with a finite number of beam splitters. Our calculation shows that the dissipation and phase fluctuation will dramatically decrease the reliability and the efficiency of communication, and even corrupt the communication. To counteract the negative effect of dissipation, we propose the balanced dissipation method, which substantially improves the reliability of the protocol at the expense of decreasing communication efficiency. Meanwhile, our theoretical derivation shows that the reliability and efficiency of communication are independent of the input state: a single photon state or a coherent state.

Keywords: dissipation, direct communication, reliability, phase fluctuation

(Some figures may appear in colour only in the online journal)

1. Introduction

Quantum information is a rapidly developing area in recent decades. One of the most important applications in quantum information is quantum communication. In 1984, Bennett and Brassard proposed the famous protocol for quantum key distribution (QKD), known as BB84 [1], which is the first practical quantum information processor [2, 3]. In the BB84 protocol, the security of the protocol is guaranteed using a single photon sent by Alice. For a high loss or an imperfect single photon state, Hwang proposed a decoy-pulse method to guarantee security under photon-number-splitting attack for BB84 [4]. Recently, A Rubenok proposed a new QKD protocol that is immune to attack on the vulnerabilities of single-photon detectors [5]. Another celebrated QKD protocol is E91 [6], which is based on quantum entanglement. At same time, using the electromagnetic field amplitudes of 'non-classical' light beams (squeezed or entangled light) for QKD also attracts much attention [7–12].

Recently, Salih *et al* proposed a protocol to realize direct counterfactual communication (no need for a prior quantum key distribution) [13] based on previous work [14], which showed how to make an interaction-free measurement [15–17]. In [13], the 'chained' quantum Zeno effect and interference of optical paths are used to achieve information transmission between Alice and Bob without any photon traveling between them, by using a single photon source. However, in order to have direct communication, a large number of perfect beam splitters (BSs) (8000 for 90% efficiency [13]) and no dissipation in all paths are required.

In [13], the authors considered the effects of two kinds of imperfection and one source of noise on the performance of counterfactual communication. One of the imperfections arises from the sensitivity of the detectors, which only affects the efficiency of communication and does not cause detection

errors. Another imperfection arises from the inaccuracy of θ (with an error $\Delta\theta$), which presents the transmittivity and reflectivity of a BS with 'transmittivity' + 'reflectivity' = 1. Please note that they still assumed that there is no dissipation or phase fluctuation in the devices (BSs, mirrors and field paths). The noise in [13] results from the partial transmission channel being blocked by an object other than Bob's, and does not result from the phase fluctuation or the dissipation in the whole direct communication protocol. However, in a real experiment, the finite number of BSs (usually fewer BSs is better), the dissipation (including the BSs themselves) and the phase fluctuation of the paths could not be avoided [18–20]. Our simulation results show that the dissipation and phase fluctuation have a great influence on the reliability of communication; for example, 1% dissipation in each field path can crash the communication protocol when $M = 20$ and $N = 50$; see figure 2.

Here we consider the effect of the dissipation and the phase fluctuation on the direct communication, and analyze how the reliability of the direct communication can be preserved. In section 2, taking into consideration the finite number of BSs, the dissipation and the phase fluctuation, we theoretically derive the transmission matrix between the input operators and the output operators, which is independent of the input states. In section 3, a numerical simulation is carried out to show the effects of the dissipation and the finite number of BSs. To improve the communication for a finite number of BSs and for dissipation, we propose the balanced dissipation method. The phase fluctuation effect is analyzed in section 4, and an example is given to shown how the finite BSs, the dissipation and the phase fluctuation affect the communication. In section 5 we give the conclusions.

2. The theoretical result with the dissipation and phase fluctuation effect

Consider the same setup as in [13], shown in figure 1(a), which is composed of two chains of BSs, the inner chain and the outer chain. The two chains are formed by $(M-1)$ and $(N-1)$ head–tail connected Mach–Zehnder interferometers (MZIs) [13]. Alice and Bob can use the setup to have information communication with a single photon field (or a coherent field) source. The outer chain contains M BSs (green color) with the same reflectivity $R = \cos^2\theta_M$ where $\theta_M = \pi/(2M)$ and $(M-1)$ mirrors (black color in figure 1(a)), which are in the hands of Alice. Each inner chain is formed by N BSs (in blue color) with the same reflectivity of $R = \cos^2\theta_N$ where $\theta_N = \pi/2N$ and $2(N-1)$ mirrors. The reflectivity of all the mirrors is 100% without the dissipation. The inner chain (figure 1(b)) has two parts, the BSs (blue color) and half of its mirrors in the hands of Alice and the other half of the mirrors in the hands of Bob. From the blue color BSs to the mirrors in Bob's hands, the field needs to pass through the transmission channel, which is publically accessible. Bob can block the paths in his hands by inserting blocks (small red color rectangles). The two outputs of each

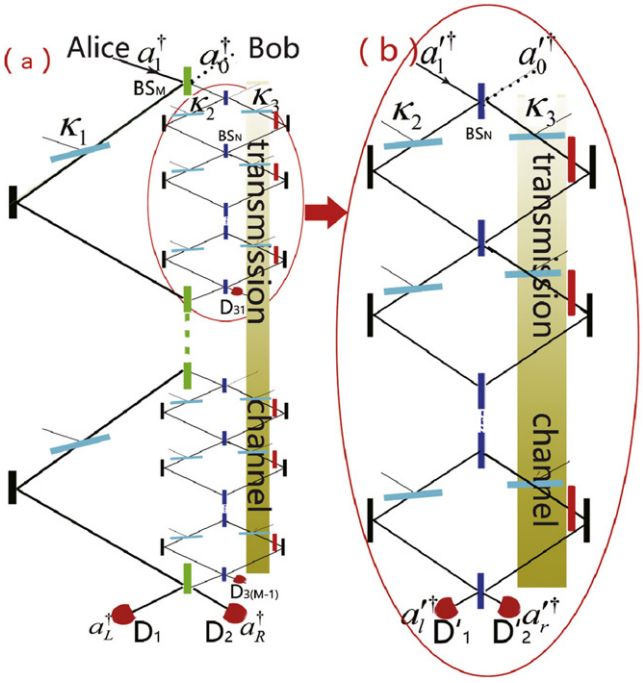

Figure 1. The scheme of direct communication.

inner chain go to the outer chain and detector D_{3i}, respectively. Alice sends out her field, a single photon; Bob can choose to insert his blocks in the paths in his side or not, and Alice measures the counting received by the two detectors, D_1, and D_2. For no dissipation and infinite M and N, when Bob inserts or does not insert his blocks, Alice sending one photon out will see D_2 or D_1 click (perfect 100% detection probability). Hence, Alice will know whether Bob inserts or does not insert the blocks.

In a real experiment, the dissipation (including the BSs and mirrors themselves) and the phase fluctuation of the paths could not be avoided. Here we group all the paths in figure 1(a) into three groups, left (paths at the left line), middle (paths in the middle line) and right (paths in the right line). We assume the dissipation of each path in the left group is the same (κ_1), the dissipation of each path in the middle group is the same (κ_2) and the dissipation of each path in the right group is the same (κ_3). If Bob choose to insert blocks in his paths, we have $\kappa_3 = 1$. The dissipation in each path can be theoretically simulated by adding a BS in the corresponding path, as shown in figure 1 by the light cyan color, and the reflected energy is proportional to the intensity dissipation, κ_i. The dissipation in a path can be theoretically calculated by multiplying by a factor of $\sqrt{1-\kappa}$. Therefore, for example, the dissipation of one MZI in the inner chain can be represented by a matrix $\begin{bmatrix} \sqrt{1-\kappa_2} & 0 \\ 0 & \sqrt{1-\kappa_3} \end{bmatrix}$. The effect of the phase difference between the two paths of each MZI in the inner chain (which is random), φ, can be represented by $M_P = \begin{bmatrix} 1 & 0 \\ 0 & e^{i\varphi} \end{bmatrix}$. Thus, the dissipation and phase fluctuation of one MZI in the inner chain can be represented by a matrix,

$\begin{bmatrix} \sqrt{1-\kappa_2} & 0 \\ 0 & e^{i\varphi}\sqrt{1-\kappa_3} \end{bmatrix}$. The modes reflected by each added BS (for dissipation) are orthogonal to each other, and they are in vacuum for no input field. Therefore, we can treat all thereflected modes as one reservoir. The input field, $a_1^\dagger$ (together with two vacuum inputs ${a_0}^\dagger$ and ${a_0'}^\dagger$), is transformed into two outputs, $a_L^\dagger$ and $a_R^\dagger$, at $D_{1,2}$, the modes $a_{3i}^\dagger$ at D_{3i} and the reservoir modes $a_{res}^\dagger$ (due to dissipation and blocks).

2.1. The transmission matrix of the inner chain

To calculate the whole protocol, first, let us analyze the transmission matrix of the inner chain. The incident field of the inner chain (see figure 1(b)) is denoted by ${a_1'}^\dagger$, the input vacuum is denoted by ${a_0'}^\dagger$ and two outputs are denoted by ${a_1'}^\dagger$ and ${a_r'}^\dagger$. Due to the dissipation, some photons go to the reservoir associated with the inner chain. Thus, the input ${a_1'}^\dagger$ (the vacuum ${a_0'}^\dagger$ has no contribution to the output) is transmitted into ${a_1'}^\dagger$, ${a_r'}^\dagger$ and ${a_{res}'}^\dagger$ with

$$a_1'^\dagger \to M_{11}' a_1'^\dagger + M_{21}' a_r'^\dagger + M_{res}' {a_{res}'}^\dagger \tag{1}$$

where ${a_{res}'}^\dagger$ is the creation operator of photons in the reservoir associated with the inner chain, and M_{11}', M_{21}' and M_{res}' are transmission coefficients with $|M'_{11}|^2 + |M'_{21}|^2 + |M'_{res}|^2 = 1$ due to the photon number conservation. The two coefficients, M_{11}' and M_{21}', are calculated in appendix A,

$$M_{11}' = \begin{bmatrix} 1 & 0 \end{bmatrix} \begin{bmatrix} \cos\theta_N & -\sin\theta_N \\ \sin\theta_N & \cos\theta_N \end{bmatrix} \times \prod_{j=1,,,N-1} \begin{bmatrix} \sqrt{1-\kappa_2}\cos\theta_N & -\sqrt{1-\kappa_2}\sin\theta_N \\ e^{i\varphi_{mj}}\sqrt{1-\kappa_3}\sin\theta_N & e^{i\varphi_{mj}}\sqrt{1-\kappa_3}\cos\theta_N \end{bmatrix} \times \begin{bmatrix} 1 \\ 0 \end{bmatrix} \tag{2a}$$

$$M_{21}' = \begin{bmatrix} 0 & 1 \end{bmatrix} \begin{bmatrix} \cos\theta_N & -\sin\theta_N \\ \sin\theta_N & \cos\theta_N \end{bmatrix} \prod_{j=1,,,N-1} \times \begin{bmatrix} \sqrt{1-\kappa_2}\cos\theta_N & -\sqrt{1-\kappa_2}\sin\theta_N \\ e^{i\varphi_{mj}}\sqrt{1-\kappa_3}\sin\theta_N & e^{i\varphi_{mj}}\sqrt{1-\kappa_3}\cos\theta_N \end{bmatrix} \begin{bmatrix} 1 \\ 0 \end{bmatrix} \tag{2b}$$

where φ_{mj} is the relative phase in the mth outer chain and jth inner chain, and follows the random normal distribution $(P(\varphi_{mj}) = \frac{1}{\sqrt{2\pi}\Delta_{inner}} \exp\left(-\frac{{\varphi_{mj}}^2}{2\Delta_{inner}^2}\right)$; Δ_{inner} is the phase fluctuation of the inner chain). Here we assume that the phase fluctuation of each inner chain is the same, Δ_{inner}.

2.2. The transmission matrix of the whole protocol

The inner chain is one of the two paths of each MZI in the outer chain. The input field of the inner chain comes from the outer chain. The left outputs of the inner chain will go to the outer chain, and the right outputs (here indicated with ${a^\dagger}_{3i}$) will be detected by Alice with detector D_{3i}; see figure 1(a). The final outputs of the outer chain, $a_R^\dagger$ and $a_L^\dagger$, will be detected by D_1 and D_2 in Alice's hands. Using the method discussed above, we can obtain the total transformation for the whole protocol; see appendix B.

$$a_1^\dagger \to M_1 a_L^\dagger + M_2 a_R^\dagger + \sum_i^{M-1} M_{3i} a_{3i}^\dagger + M_{res}\, a_{res}^\dagger \tag{3}$$

where

$$M_1 = \begin{bmatrix} 1 & 0 \end{bmatrix} \begin{bmatrix} \cos\theta_M & -\sin\theta_M \\ \sin\theta_M & \cos\theta_M \end{bmatrix} \times \prod_{k=1,2,,,M-1} \left\{ \begin{bmatrix} e^{i\phi_k}\sqrt{1-\kappa_1} & 0 \\ 0 & M'_{11} \end{bmatrix} \times \begin{bmatrix} \cos\theta_M & -\sin\theta_M \\ \sin\theta_M & \cos\theta_M \end{bmatrix} \right\} \begin{bmatrix} 1 \\ 0 \end{bmatrix} \tag{4a}$$

$$M_2 = \begin{bmatrix} 0 & 1 \end{bmatrix} \begin{bmatrix} \cos\theta_M & -\sin\theta_M \\ \sin\theta_M & \cos\theta_M \end{bmatrix} \times \prod_{k=1,2,,,M-1} \left\{ \begin{bmatrix} e^{i\phi_k}\sqrt{1-\kappa_1} & 0 \\ 0 & M'_{11} \end{bmatrix} \times \begin{bmatrix} \cos\theta_M & -\sin\theta_M \\ \sin\theta_M & \cos\theta_M \end{bmatrix} \right\} \begin{bmatrix} 1 \\ 0 \end{bmatrix} \tag{4b}$$

$$M_{3i} = \begin{bmatrix} 0 & 1 \end{bmatrix} \begin{bmatrix} \cos\theta_N & -\sin\theta_N \\ \sin\theta_N & \cos\theta_N \end{bmatrix} \times \prod_{j=1,,,N-1} \begin{bmatrix} \sqrt{1-\kappa_2}\cos\theta_N & -\sqrt{1-\kappa_2}\sin\theta_N \\ e^{i\varphi_{mj}}\sqrt{1-\kappa_3}\sin\theta_N & e^{i\varphi_{mj}}\sqrt{1-\kappa_3}\cos\theta_N \end{bmatrix} \times \begin{bmatrix} M_{i\,(inner)} \\ 0 \end{bmatrix} \tag{4c}$$

$$M_{i\,(inner)} = \begin{bmatrix} 0 & 1 \end{bmatrix} \begin{bmatrix} \cos\theta_M & -\sin\theta_M \\ \sin\theta_M & \cos\theta_M \end{bmatrix} \times \prod_{k=1,2,,,i-1} \left\{ \begin{bmatrix} e^{i\phi_k}\sqrt{1-\kappa_1} & 0 \\ 0 & M'_{11} \end{bmatrix} \times \begin{bmatrix} \cos\theta_M & -\sin\theta_M \\ \sin\theta_M & \cos\theta_M \end{bmatrix} \right\} \begin{bmatrix} 1 \\ 0 \end{bmatrix} \tag{4d}$$

and (due to energy conservation)

$$M_{res} = \sqrt{1 - |M_1|^2 - |M_2|^2 - \sum_{i=1}^{M-1} |M_{3i}|^2} \tag{5}$$

where ϕ_k is the phase fluctuation of the left path in the kth outer chain, and follows the random normal distribution $(P(\phi_k) = \frac{1}{\sqrt{2\pi}\Delta_{outer}} \exp\left(-\frac{{\phi_k}^2}{2\Delta_{outer}^2}\right)$; Δ_{outer} is the phase fluctuation of the left path of the outer chain).

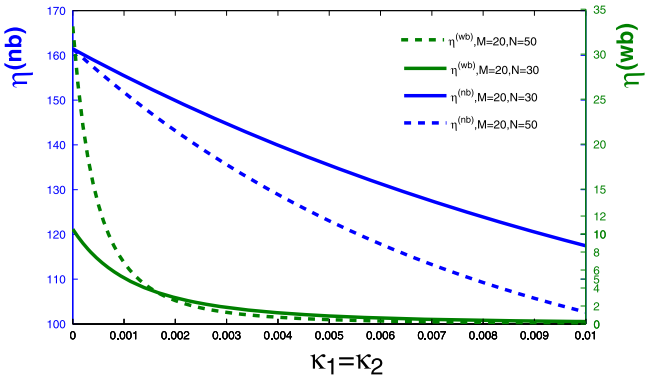

Figure 2. The reliability as a function of the dissipation, $\kappa_1 = \kappa_2$, where the transmission channel's dissipation is $\kappa_3 = 5\kappa_2$ The figure shows that $\eta^{(\mathrm{wb})}w$ sharply decreases with a dissipation increase.

2.3. Output field

In the above derivation, we use the operator transformation, while the input state is not specified. That is to say, we can use any input state for further derivation. We assume that the state of the input field can be written in the form

$$\left|\psi_i\right\rangle = f\left(a_1^\dagger\right)|\{0\}\rangle \tag{6}$$

with $f(x)$ is an arbitrary function of the argument, x. Based on equation (3), the state of the output fields can be written as

$$\left|\psi_f\right\rangle = f\left(M_1 a_{\mathrm{L}}^\dagger + M_2 a_{\mathrm{R}}^\dagger + \sum_i^{M-1} M_{3i} a_{3i}^\dagger + M_{\mathrm{res}}\, a_{\mathrm{res}}^\dagger\right)|\{0\}\rangle. \tag{7}$$

If the input state is a single photon, we have $f(a_1^\dagger) = a_1^\dagger$, and the final state is

$$\begin{aligned}\left|\psi_f\right\rangle &= M_1 a_{\mathrm{L}}^\dagger + M_2 a_{\mathrm{R}}^\dagger + \sum_i^{M-1} M_{3i} a_{3i}^\dagger + M_{\mathrm{res}}\, a_{\mathrm{res}}^\dagger \;|\{0\}\rangle \\ &= \left|M_1, M_2, M_{31} \ldots M_{3(M-1)}, M_{\mathrm{res}}\right\rangle.\end{aligned} \tag{8}$$

For a coherent state input we have $f(a_1^\dagger) = \mathrm{e}^{-|\alpha|^2/2}\mathrm{e}^{\alpha a_1^\dagger}$; the final state is

$$\begin{aligned}\left|\psi_f\right\rangle &= \mathrm{e}^{-|\alpha|^2/2}\mathrm{e}^{\alpha\left(M_1 a_{\mathrm{L}}^\dagger + M_2 a_{\mathrm{R}}^\dagger + \sum_i^{M-1} M_{3i} a_{3i}^\dagger + M_{\mathrm{res}}\, a_{\mathrm{res}}^\dagger\right)}|\{0\}\rangle \\ &= \left|M_1\alpha\right\rangle_1 \left|M_2\alpha\right\rangle_2 \left|M_{31}\alpha\right\rangle_{31} \ldots \\ &\quad \times \left|M_{3(M-1)}\alpha\right\rangle_{3(M-1)} \left|M_{\mathrm{res}}\,\alpha\right\rangle_{\mathrm{res}}\end{aligned} \tag{9}$$

In the above, $|M_1|^2$, $|M_2|^2$ and $|M_{3i}|^2$ are the probabilities of a photon for the single photon input (or of intensities for the coherent state input) detected by D_1, D_2 and D_{3i}, respectively, and $|M_{\mathrm{res}}|^2$ is the probability of a photon (or intensity) leaked out to the reservoir (some in Alice's hands and others in the transmission channel). Note that D_1, D_2 and D_{3i} ($i = 1, \ldots, M-1$) are in the hands of Alice. From equations (8) and (9) we know that the proportions of field energy to each detector and the reservoir are independent of the input state. If we consider the ratios, we can obtain the same result with a single photon or by using a coherent state. For s single photon input, only one detector can have a click, or all detectors have no click if the one photon goes to the reservoir. If no click, we can throw away this communication (no information exchanged between Alice and Bob). For the single photon input there is no photon in the transmission channel when D_1 or D_2 has a click (counterfactual), while for the coherent state input there are photons in the transmission channel (not counterfactual). For the two different inputs, the detection probabilities (efficiencies) of D_1 and D_2 (W_1 and W_2) are the same, and also their ratios (reliabilities). In the experiment, in order to make the optical lengths for the two paths in each MZI equal, coherent light is always used for the adjustment of the optical lengths.

For finite N and M, in order to measure how good the direct communication is, we introduce two quantities. (1) *The probabilities* (also called efficiencies), $W_1^{(\mathrm{nb})}$ (together with $W_2^{(\mathrm{nb})}$) for no blocks and $W_2^{(\mathrm{wb})}$ ($W_1^{(\mathrm{wb})}$) for with blocks, which represent the efficiency of the direct communication. Large $W_1^{(\mathrm{nb})}$ and $W_2^{(\mathrm{wb})}$ mean high efficient usage of the input photon for the communication. (2) *The reliabilities*, $\eta^{(\mathrm{nb})} = W_1^{(\mathrm{nb})}/W_2^{(\mathrm{nb})}$ for no blocks and $\eta^{(\mathrm{wb})} = W_2^{(\mathrm{wb})}/W_1^{(\mathrm{wb})}$ for with blocks, which represent how reliable the communication is. For no blocks we want $W_2^{(\mathrm{nb})} \to 0$, while for with blocks we want $W_1^{(\mathrm{wb})} \to 0$, so that Alice immediately knows that Bob inserts (or does not insert) his blocks when she sees the click of D_2 (or D_1). The larger $\eta^{(\mathrm{nb})}$ and $\eta^{(\mathrm{wb})}$ are, the more reliable the communication is. For a perfect communication, we have $W_1^{(\mathrm{nb})} = 1$ and $\eta^{(\mathrm{nb})} = \infty$ for no blocks and $W_2^{(\mathrm{wb})} = 1$ and $\eta^{(\mathrm{wb})} = \infty$ for with blocks. The higher the values for the four quantities (two efficiencies and two reliabilities), the better the communication is.

In a real experiment, the dissipation also has fluctuation. We have assumed a Gaussian dissipation fluctuation, $P(\kappa) = \frac{1}{\sqrt{2\pi}\Delta_i}\exp\left(-\frac{(\kappa-\kappa_i)^2}{2{\Delta_i}^2}\right)$, with a width of $\Delta_i = 0, 0.1\kappa_i$, and our simulation found that the dissipation fluctuation has almost no effect, because the phase fluctuation is much more important than the dissipation fluctuation. That is to say, compared with the phase fluctuation, the dissipation fluctuation is negligible.

3. Numerical result of the dissipation effect and balanced dissipation method

In this section, we consider only the effect of dissipation, by setting the phase fluctuations $\varphi_{mj} = \phi_k = 0$. Here we set the energy of the input state to be unity. We discuss the proportions of energy entering each detector. In the following diagrams, the energies received by detectors D_1, D_2 and D_{3i} are labeled by W_1, W_2 and W_{3i}, while the dissipated energy by W_{res}. Please note that $\mathrm{W_1} + \mathrm{W_2} + \sum_i \mathrm{W_{3i}} + \mathrm{W_{res}} = \mathrm{W_{input}} = 1$ as the input energy is set to unity.

To demonstrate the importance of the dissipation effect in direct communication, we plot figure 2, the reliability as a function of the dissipation, $\kappa_1 = \kappa_2$, where the transmission channel's dissipation is $\kappa_3 = 5\kappa_2$. From the two dashed curves, $M = 20$, $N = 50$ (blue for $\eta^{(nb)}$, green for $\eta^{(wb)}$), we can clearly see that $\eta^{(wb)}$ sharply decreases with a dissipation increase. When $\kappa_1 = \kappa_2 = 3 \times 10^{-3}$, the figure shows $\eta^{(wb)} \simeq 1$, which means that Bob cannot transmit the 'block' information to Alice. Comparing the dashed curve and solid curve, we know that the reliability decreases faster when N is larger. However, to realize direct communication, $N \to \infty$ is needed [13]. Therefore, in order to put [13] into a more realistic framework, investigations of the effect of dissipation and phase fluctuation are very necessary.

3.1. No blocks

If Bob does not insert his blocks, the interference occurs between the two paths of each MZI in the inner chain (figure 1(b)). Without dissipation, no blocks will result in complete interference, so that no photon enters D_1' (photon completely entering D_2'). If we have the same dissipation (balanced dissipation) for the two paths of each MZI in the inner chain, $\kappa_2 = \kappa_3$, complete interference can also be achieved. For balanced dissipation, we still have complete interference in the inner chain, and there is no photon entering D_1', while the probability of the photon entering D_2' decreases with increasing dissipation. In figure 2, we plot the probability ratio W_2'/W_1' versus κ_2 with $\kappa_3 = 10^{-3}$, $N = 12$ and no blocks. Please note the peak (infinity) at $\kappa_2 = \kappa_3$ due to $W_1' = 0$, because of the complete interference. For no blocks, with balanced dissipation for each MZI of the inner chain ($\kappa_2 = \kappa_3$), the photon entering the inner chain will not return to the outer chain ($W_1' = 0$), which is independent of N (as for no dissipation). Therefore, balanced dissipation in the inner chain will not affect the outer chain. That is to say, for $\kappa_2 = \kappa_3$ and no block, the ratio of the photon probabilities (efficiencies) entering D_1 and D_2 is only determined by M, and is independent from the dissipation in the paths of the left group, κ_1, the same as the case of no dissipation. The ratio (also the reliability) is $\eta^{(nb)} = \cos^2(\pi/2M)/\sin^2(\pi/2M)$ for no blocks and balanced dissipation; see figure 4(a).

3.2. With blocks ($\kappa_3 = 1$)

Let us first consider the case without dissipation. In figure 4(b), we plot the reliability, $\eta^{(wb)}$, when Bob blocks his mirrors versus N and M. Please note that $\eta^{(nb)}$ (no blocks) does not depend on N, and $\eta^{(wb)}$ (with blocks) always decreases with M for fixed N. Larger M gives larger $\eta^{(nb)}$ (no blocks), while larger N gives larger $\eta^{(wb)}$ (with blocks) for fixed M. In principle, as both M and N tend to infinity (the two ratios both go to infinity), the detection probability of the photon by D_1 or D_2 goes to 100%, and consequently direct communication (counterfactual for single photon input) between Alice and Bob is achieved [13].

Now let us consider the influence of the dissipation. The energy dissipations in the three path groups (indicated in figure 1(a)) are denoted by κ_1, κ_2 and κ_3. In figure 5, we plot the reliability, $\eta^{(wb)}$ (with blocks), versus N and M, with $\kappa_2 = \kappa_3 = 10^{-4}$ (balanced dissipation) and $\kappa_1 = 3\kappa_2$. Please note that the loss of the best quality BS currently available is at the order of 10^{-4} to 10^{-5}. When the dissipation is included, we find that $\eta^{(nb)}$ (no blocks) still increases with M under balanced dissipation in the inner chain, equivalent to no dissipation (see figure 4a). For no blocks and under balanced dissipation ($\kappa_2 = \kappa_3$), the reliability ($\eta^{(nb)}$) does not depend on the dissipation ($\kappa_{1,2,3}$), and the efficiency ($W_1^{(nb)}$) only depends on κ_3. However, the reliability $\eta^{(wb)}$ increases, and then decreases with N if M is larger than a certain value (see figure 5), due to the dissipation. In other words, for the large M, N region, the reliability $\eta^{(wb)}$ decreases with M and N. Here we ask ourselves 'Can we increase the reliability ($\eta^{(wb)}$) when the dissipation is included?'

3.3. Improvement of the reliability $\eta^{(wb)}$ by the balanced dissipation method

When Bob inserts the blocks in his paths, from the above analysis we know that some photons will be lost due to the blocks for finite N (note no photon loss only for infinite N and no dissipation). The portion of the photon probability entering the inner chain will return to the outer chain, which results in interference between the paths of the left group (the left paths of the out chain) and the paths of the middle group (the left paths of the inner chain) at the BSs of the outer chain (each MZI of the outer chain). Thus, as result of unbalanced interference between the left path and middle path, the output state at D_1 is not the vacuum for finite M, even with no dissipation. As discussed for no blocks, the use of balanced dissipation ($\kappa_2 = \kappa_3$) in the inner chain makes the inner chain equivalent to no dissipation. Can we use the idea of balanced dissipation in the outer chain to obtain high reliability $\eta^{(wb)}$ (with blocks), even $\eta^{(wb)} \to \infty$? The answer is yes. The interference at these BSs of the outer chain is dependent on κ_1; that is to say, the interference can be adjusted by κ_1, and so can the output at D_1. When Bob blocks his paths ($\kappa_3 = 1$), the proportion of photons returned to the outer chain from the inner chain is $\cos^2\theta_N\left(\sqrt{1-\kappa_2}\cos\theta_N\right)^{2(N-1)}$, which can be viewed an equivalent dissipation in the paths of the middle group, $\kappa_2' = 1 - \cos^2\theta_N\left(\sqrt{1-\kappa_2}\cos\theta_N\right)^{2(N-1)}$. If we introduce a dissipation in the paths of the left group (outer chain),

$$\kappa_1 = 1 - \cos^2\theta_N\left(\sqrt{1-\kappa_2}\cos\theta_N\right)^{2(N-1)} \tag{10}$$

we can achieve a complete interference at the BSs of the MZIs of the outer chain, which results in the vacuum state for the output at D_1, and consequently we have $\eta^{(wb)} \to \infty$ (highest reliability). Please note that κ_2 can be zero (no dissipation) in equation (10). By adjusting the dissipation, Alice and Bob with finite N and M can have a better communication compared to the case of no dissipation. In figure 6, we plot the influence of κ_1 and κ_2 on $\eta^{(wb)}$ for $N = 12$

Table 1. The efficiency (the photon probability entering D_2), $W_2^{(wb)}$, and the total photon probability in all paths in the transmission channel, $W_{Tr}^{(wb)}$, for different dissipations and M, N, when Bob inserts the blocks ($\kappa_3 = 1$). With the balanced dissipation method, we have $W_1^{(wb)} = 0$; $\eta^{(wb)} = \infty$. Please note that we can manipulate the dissipation κ_1 to maximize $\eta^{(wb)}$, which has no effect on $\eta^{(nb)}$.

M, N	No dissipation, $W_{res}^{(wb)} = 0$				Balanced dissipation, κ_1 see equation (10), $W_1^{(wb)} = 0$; $\eta^{(wb)} = \infty$							
	$\kappa_1 = \kappa_2 = 0$				$\kappa_2 = 0$				$\kappa_2 = 10^{-4}$			
	$W_2^{(wb)}$	$W_3^{(wb)}$	$\eta^{(wb)}$	$W_{Tr}^{(wb)}$	$W_2^{(wb)}$	$W_3^{(wb)}$	$W_{res}^{(wb)}$	$W_{Tr}^{(wb)}$	$W_2^{(wb)}$	$W_3^{(wb)}$	$W_{res}^{(wb)}$	$W_{Tr}^{(wb)}$
6,12	0.612	0.027	22.5	0.326	0.357	0.020	0.380	0.244	0.354	0.020	0.383	0.243
12,20	0.536	0.020	13.8	0.406	0.257	0.013	0.466	0.264	0.251	0.013	0.476	0.260
20,30	0.490	0.015	10.6	0.449	0.209	0.009	0.512	0.270	0.197	0.009	0.534	0.260
20,50	0.641	0.007	33.1	0.333	0.392	0.005	0.360	0.244	0.355	0.005	0.411	0.229
30,50	0.517	0.009	13.2	0.436	0.239	0.005	0.486	0.270	0.206	0.005	0.543	0.247
40,100	0.633	0.003	32.6	0.344	0.382	0.003	0.368	0.248	0.258	0.002	0.548	0.192

and $M = 6$, where we can see $\eta^{(wb)} \to \infty$ ($W_1 = 0$, no photon probability for D_1) when equation (10) is satisfied.

Here we would like to emphasize that $\eta^{(nb)}$ (no blocks) is not affected by κ_1, if we set the balanced dissipation in the inner chain $\kappa_3 = \kappa_2$ (including $\kappa_3 = \kappa_2 = 0$), because there is no photon probability from the inner chain back to the outer chain. Therefore, we can manipulate the dissipation κ_1 to maximize $\eta^{(wb)}$ (with blocks), which has no effect on $\eta^{(nb)}$ (no blocks). By using balanced dissipation (for both inner and outer chains), we can improve the communication between Alice and Bob with a few N and M.

However, the benefit of this method for the reliability improvement is not free. What is the expense? The input photon will go to D_1, D_2, D_{3s} and the reservoirs, with probabilities $W_1^{(wb,nb)}$, $W_2^{(wb,nb)}$, $W_{3s}^{(wb,nb)}$ and $W_{res}^{(wb,nb)}$, respectively (see equation (3)). In table 1, we list the probabilities with the blocks inserted. Here we focus on the efficiency (the photon probability entering D_2), $W_2^{(wb)}$. Without dissipation ($\kappa_1 = \kappa_2 = 0$), and $M = 6$, $N = 12$, the efficiency $W_2^{(wb)}$ is 62%; with the balanced dissipation method (determined by equation (10)) it decreases to 36%. The balanced dissipation can give very high reliability ($\eta^{(wb)} \to \infty$) at the expense of reducing the efficiency ($W_2^{(wb)}$); see table 1. The reduction is due to the photons lost to the reservoirs; see $W_{res}^{(wb)}$ in table 1. For large N and M, the balanced dissipation method will greatly reduce the efficiency ($W_2^{(wb)}$). Meanwhile, the photon probability to D_{3s} is small, less than 2%.

Now let us consider the total photon probability in all the transmission channels, from every BS_N to the corresponding blocks in figure 1, $W_{Tr}^{(wb)}$, which is listed in the last columns in table 1. It is clear that the balanced dissipation method can also reduce the photon probability in the transmission channel, which is another benefit of the balanced dissipation method for finite N and M.

3.4. The performance of the balanced dissipation method when the transmission channel's dissipation κ_3 is large

In the above calculation, we have assumed that the dissipation of the three kinds of field channel are tiny, such as $\kappa \approx 10^{-4}$. For a transmission channel some kilometers long, however, it is possible that κ_3 (the transmission channel's dissipation) is very large. Suppose $\kappa_3 = 0.99$, which means the photon is almost dying before it arrives on Bob's side, thus the interference of the inner chain is always broken down, no matter whether Bob inserts his blocks or not; see figure 1. Consequently, the probability of D_1, D_2 click is independent of Bob's action, and the communication fails. Please note that the success of the protocol is based on the interference: when Bob does not insert blocks, he builds the inner chain's interference (D_1' click); while if Bob does insert blocks, he destroys the inner chain's interference and builds the Zeno effect in the middle path (D_2' click). However, unbalanced dissipation ($\kappa_3 \gg \kappa_2$) of two paths will inhibit the interference, or even destroy it; see figure 3. For example, in the case of $M = 6$, $N = 12$ and $\kappa_1 = \kappa_2 = 10^{-4}$, if $\kappa_3 = 0.99$ (a very large dissipation in the transmission channel), we obtain $W_1^{(wb)} = 0.038$, $W_1^{(nb)} = 0.062$ and $W_2^{(wb)} = 0.56$, $W_2^{(nb)} = 0.57$. $W_2^{(wb)} \approx W_2^{(nb)} > W_1^{(wb)} \approx W_1^{(nb)}$, independent of Bob's action. Thus, Alice cannot obtain information.

To determine how the transmission channel's dissipation κ_3 influences the communication, in figure 7 we plot the reliability $\eta^{(nb)}$ as a function of the transmission channel's dissipation κ_3, for different M, N combinations. Here we assume that $\kappa_1 = \kappa_2 = 10^{-4}$, as the dissipation of these two paths can be suppressed technologically in Alice's laboratory. Comparing the red dotted curve ($M = 20$, $N = 30$) and cyan dashed curve ($M = 20$, $N = 50$) in figure 7, we see that decreasing N can improve $\eta^{(nb)}$, because the same unbalanced dissipation will disturb the interference more significantly if N is larger. However, for each M, N combination, there is a largest dissipation κ_3, over which the communication fails. So, a very large dissipation can crash the communication protocol [13]. For example, $\kappa_3 = 0.58$ results $\eta^{(nb)} \simeq 1$ when $M = 6$, $N = 12$.

To test the performance of the balanced dissipation method (equation (10)), we calculate the reliability and the efficiency as a function of κ_2, when $\kappa_3 = 0.3$ (a large dissipation in the transmission channel); see figure 8 (Bob inserts

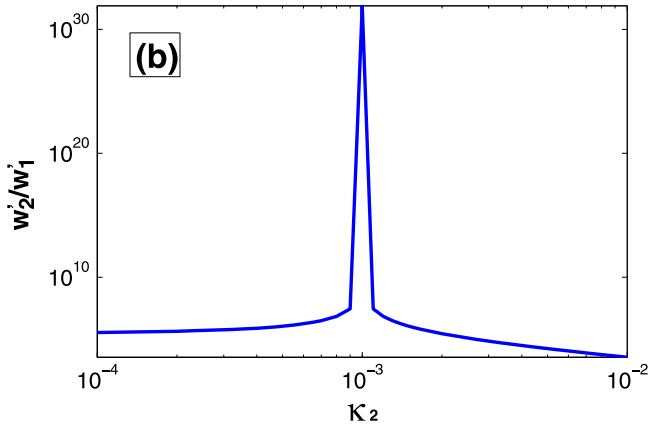

Figure 3. The effect of the dissipation, W_2'/W_1', versus κ_2 with $\kappa_3 = 10^{-3}$ and $N = 12$. If we have the same dissipation (balanced dissipation) for the two paths of each MZI in the inner chain, $\kappa_2 = \kappa_3$, complete interference can also be achieved, in which no photon enters D_1'.

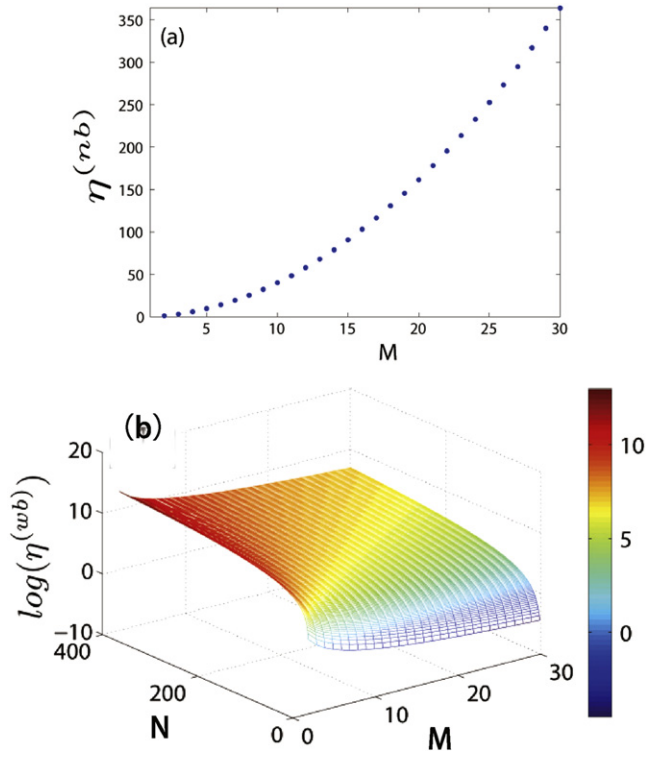

Figure 4. The reliability versus N and M without dissipation: (a) Bob does not block the paths ($\eta^{(nb)}$); (b) Bob blocks the paths $\log(\eta^{(wb)})$, which increase with M.

blocks) and figure 9 (Bob does not insert blocks). Please note that we do not let $\kappa_2 = \kappa_3$. Large κ_2 (such as $\kappa_2 = \kappa_3 = 0.3$) will result in $\kappa_1 \simeq 1$ (see equation (10)), and consequently there is no click in D_1 or D_2.

The encouraging advantage is that we have a great reliability $\eta^{(wb)} \to \infty$ when we adopt the balanced dissipation method. Meanwhile, the reliability $\eta^{(nb)} \simeq 8.0$ just has a very slight drop from $\eta^{(nb)} = 9.7$ when $\kappa_1 = \kappa_2 = 10^{-4}$. Although figures 8 and 9 have shown that the efficiencies $W_2^{(wb)}$ and

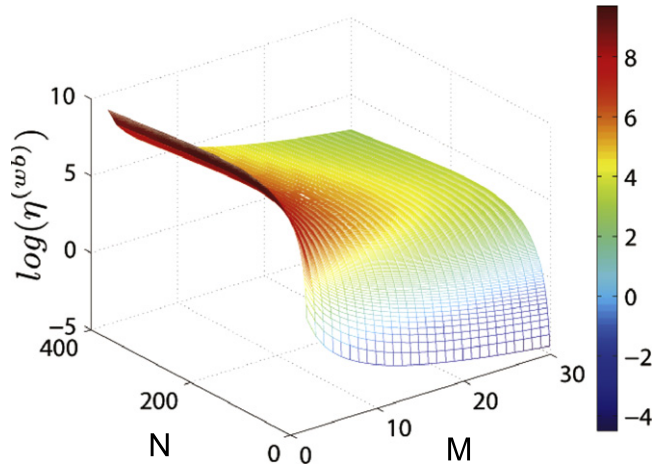

Figure 5. The reliability ($\log(\eta^{(wb)})$) versus N and M with dissipation $\kappa_2 = \kappa_3 = 10^{-4}$ and $\kappa_1 = 3\kappa_3$. For the larger M, N region, the reliability $\eta^{(wb)}$ decreases with M and N.

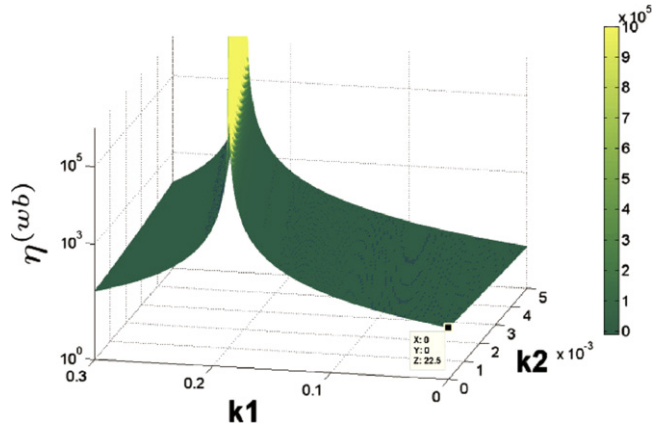

Figure 6. The influence of κ_1 and κ_2 on $\eta^{(wb)}$ for $N = 12$ and $M = 6$.

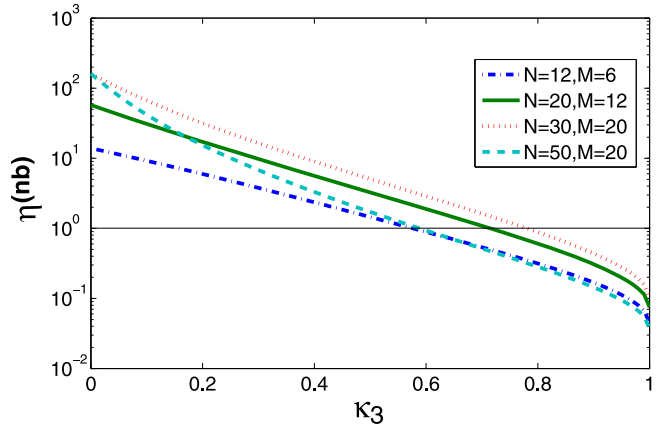

Figure 7. The reliability $\eta^{(nb)}$ versus the transmission channel's dissipation κ_3, for different M, N combinations: blue dot–dashed curve, $M = 6$, $N = 12$; green solid curve, $M = 12$, $N = 20$; red dotted curve, $M = 20$, $N = 30$; cyan dashed curve, $M = 20$, $N = 50$, with $\kappa_1 = \kappa_2 = 10^{-4}$. To realize a reliable communication, a large $\eta^{(nb)} > 1$ is needed.

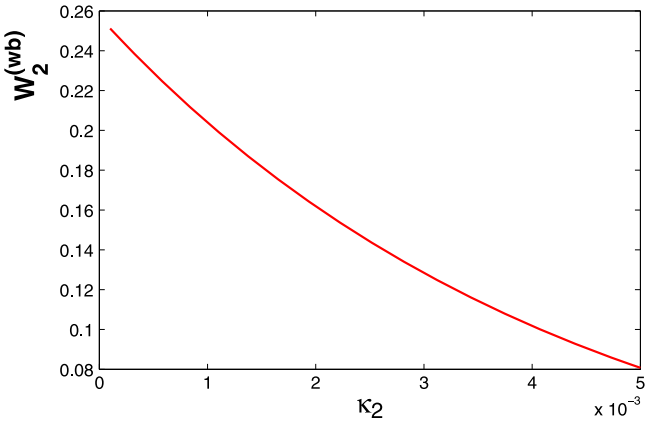

Figure 8. For the combination $M = 12$ and $N = 20$, the efficiency $W_2^{(wb)}$(Bob inserts blocks) as a function of κ_2, which can be adjusted by Alice. Here, we let $\kappa_3 = 0.3$ (a large dissipation in the transmission channel), and κ_1 following equation (10), which guarantees $\eta^{(wb)} \to \infty$.

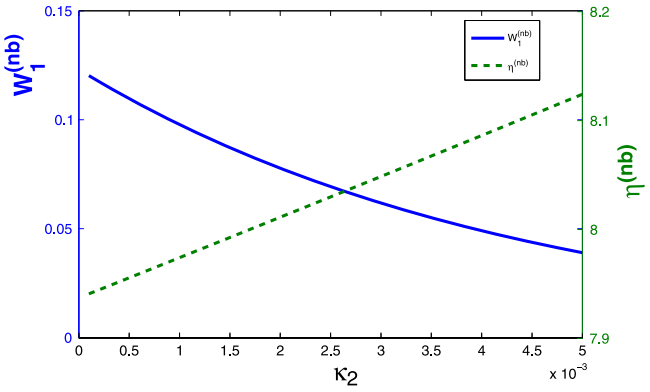

Figure 9. For the same parameter setup as figure 8 ($M = 12$, $N = 20$ and κ_1 following equation (10)), the efficiency $W_1^{(nb)}$ and $\eta^{(nb)}$ (does not insert blocks) as a function of κ_2.

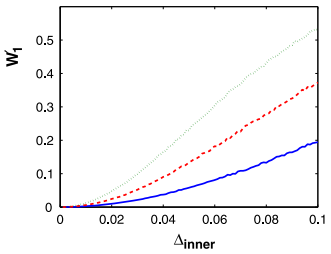

Figure 10. The output of the inner chain, W'_1, versus the phase fluctuation, Δ_{inner}, for no dissipation with $N = 20$ (blue solid curve), 50 (red dashed curve) and 100 (green dotted curve).

$W_1^{(nb)}$ have a decrease, they are still acceptable in experiment when compensation dissipation κ_2 is small. It is true that, even for a large κ_3, we can increase $\eta^{(nb)}$ further by increasing κ_2 ($\kappa_2 \to \kappa_3$), but the efficiencies $W_2^{(wb)}$ and $W_1^{(nb)}$ will decrease to zero. Therefore, the balanced dissipation method has a better performance with a small dissipation rather than a large dissipation.

4. Numerical result of the phase fluctuation effect

Now let us calculate the influence of the random phase fluctuation. For the effect of the phase fluctuation, we need to average the random phases, which are a Gaussian distribution with various widths. We use the computer to perform the average. Let first consider only the phase fluctuation by setting zero dissipation ($\kappa_1 = \kappa_2 = \kappa_3 = 0$). From the above discussion, for no blocks we know that the port to detector D_1' is a dark one, $W_1' = 0$. The phase fluctuation will disturb the interference of the inner chain MZIs, and the dark port will no longer be dark, $W_1' \neq 0$. In figure 10, we plot the photon probability W_1' versus the fluctuation width Δ_{inner}. It is clear that the leakage to the dark port D_1' (W_1') increases with the increasing of the fluctuation (Δ_{inner}) and N. In figure 10, we find that the phase fluctuation of $\Delta_{inner} = 0.05$ will result in 6%, 13% and 23% photon leakage to the previous dark port D_1' for $N = 20$, 50 and 100, respectively. Note that 6% leakage might destroy the direct communication.

For the whole protocol, we calculate the efficiencies ($W_1^{(nb)}$ and $W_2^{(wb)}$) and the reliabilities ($\eta^{(nb)}$, $\eta^{(wb)}$) versus the phase fluctuation Δ_{inner} in figure 11, with balanced dissipation ($\kappa_2 = \kappa_3 = 10^{-4}$ and κ_1 determined by equation 10) for different N and M combinations. Here we assume that $\Delta_{outer} = 2\Delta_{inner}$. In figure 11, we find that the efficiency $W_2^{(wb)}$ shows almost no decrease, but the reliability $\eta^{(wb)}$ decreases very quickly with the phase fluctuation Δ_{inner}.

For the case of $M = 6$ and $N = 12$ with no phase fluctuation and no dissipation, we know $\eta^{(wb)} = 22.5$ from table 1, and $\eta^{(nb)} = 13.9$ from figure 4(a). With the balanced dissipation method, the red curve in figure 11(a) tells us that $\eta^{(wb)} \gg 100$ for small phase fluctuation ($\Delta_{inner} < 0.01$), and $\eta^{(nb)} \approx 13.9$ (almost the same); see the red curve in figure 11(b). That is to say, for small phase fluctuation, the balanced dissipation can also greatly improve the reliability of the communication $\eta^{(wb)}$, and keep $\eta^{(nb)}$ almost the same. For $M = 30$ and $N = 50$ with no phase fluctuation and no dissipation, we know that $\eta^{(wb)} = 13.2$ from table 1, and $\eta^{(nb)} = 364$ from figure 3(a). The green curve in figure 11(a) (under balanced dissipation) tells us that $\eta^{(wb)} \gg 100$ for small phase fluctuation ($\Delta_{inner} < 0.008$). Meanwhile, we still have $\eta^{(nb)} \approx 364$ (almost the same); see the green curve in figure 11(b). Thus, the balanced dissipation method makes the realization of direct communication practical in experiment. Please note that, for large phase fluctuation, the advantage of the balanced dissipation method to improve the reliability of $\eta^{(wb)}$ will disappear. It is predictable that the communication will fail for large phase fluctuation.

5. Conclusion

We have numerically simulated the effect of the dissipation and the phase fluctuation with a finite number of BSs in a direct communication protocol. Our calculation shows that, taking into consideration the dissipation, the reliability decreases with M and N in the larger M, N region. To

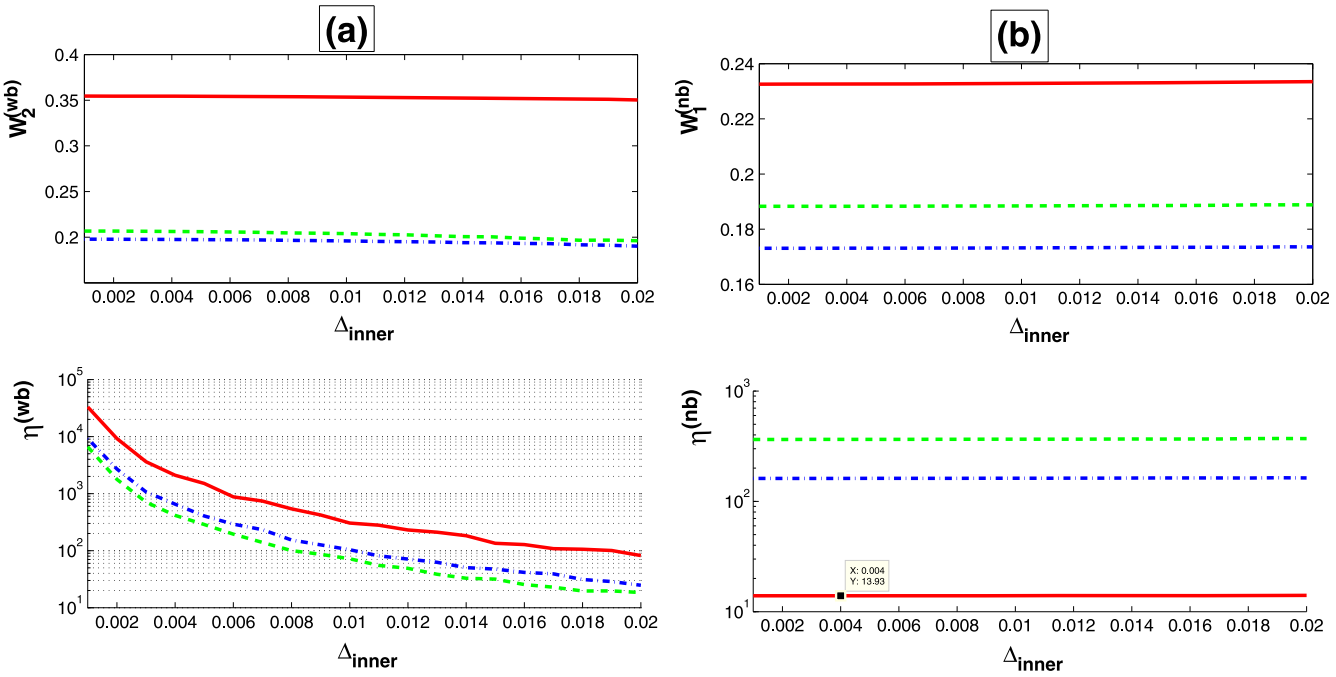

Figure 11. The efficiencies (photon detection probabilities) and reliabilities, (a) $W_2^{(wb)}$, $\eta^{(wb)}$ (Bob does insert blocks) and (b) $W_1^{(nb)}$, $\eta^{(nb)}$ (Bob does not insert blocks), versus the phase fluctuation Δ_{inner}: red solid curve for $M = 6$, $N = 12$, blue dot-dashed curve for $M = 20$, $N = 30$, and green dashed for $M = 30$, $N = 50$.

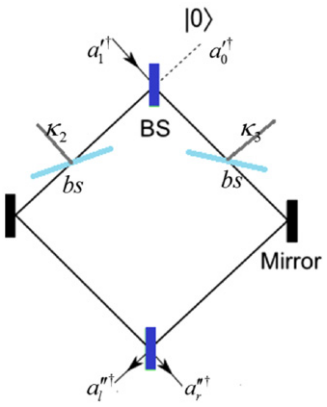

Figure 12. MZI.

counteract the negative effect of dissipation , we proposed the balanced dissipation method, which substantially improves the reliability of the protocol at the expense of decreasing communication efficiency. Our work puts the direct communication protocol into a more realistic framework. Our theoretical derivation, based on operator transmission (from input field operator to output operators), shows that the probabilities of the field going into the D_1 and D_2 are independent of the input state. Thus, the reliability and efficiency of communication using a single photon source are same as those using a coherent source. For single photon input, we need to use single photon detectors, while for coherent state input, we need intensity detectors. In experiments, the coherent state is much easier to produce and to control compared with the single photon state, and can be used to prove the direct communication property of the protocol, except the counterfactual property.

Acknowledgments

This work was supported by the National Basic Research Program of China (grants 2012CB921601 and 2011CB922203) and the National Natural Science Foundation of China (grants 11174026 and U1330203).

Appendix A. The inner chain

Let us consider one of the MZIs in the inner chain, for example the first one; see figure 12. The inputs are $a_1'^{\dagger}$ and $a_0'^{\dagger}$, while the outputs are $a_1''^{\dagger}$ and $a_r''^{\dagger}$ with two dissipations κ_2 and κ_3. We can use the matrix method to obtain the outputs. The two BSs can be expressed by the same matrix $\begin{bmatrix} \cos\theta & -\sin\theta \\ \sin\theta & \cos\theta \end{bmatrix}$. The two dissipations and the phase fluctuation can be expressed by the matrixes $\begin{bmatrix} 1 & 0 \\ 0 & e^{i\varphi_{mj}}\sqrt{1-\kappa_3} \end{bmatrix}$, and $\begin{bmatrix} \sqrt{1-\kappa_2} & 0 \\ 0 & 1 \end{bmatrix}$ where φ_{mj} is the relative phase in the mth outer chain and jth inner chain, and follows the random normal distribution $(P(\varphi_{mj}) = \frac{1}{\sqrt{2\pi}\Delta_{inner}} \exp\left(-\frac{\varphi_{mj}^2}{2\Delta_{inner}^2}\right)$; Δ_{inner} is

the phase fluctuation of the inner chain). Here we assume that the phase fluctuation of each inner chain is the same, Δ_{inner}.

The relation between the output and the inputs can be written as

$$\begin{aligned}\begin{pmatrix} a_1''^{\dagger} \\ a_r''^{\dagger} \end{pmatrix} &= \begin{bmatrix} \cos\theta_N & -\sin\theta_N \\ \sin\theta_N & \cos\theta_N \end{bmatrix} \left\{ \begin{bmatrix} \sqrt{1-\kappa_2} & 0 \\ 0 & e^{i\varphi_{mj}}\sqrt{1-\kappa_3} \end{bmatrix} \right. \\ &\quad \left. \times \begin{bmatrix} \cos\theta_N & -\sin\theta_N \\ \sin\theta_N & \cos\theta_N \end{bmatrix} \right\} \begin{pmatrix} a_1'^{\dagger} \\ a_0'^{\dagger} \end{pmatrix} \\ &= \begin{pmatrix} \left(\sqrt{1-\kappa_2}\cos^2\theta_N - e^{i\varphi_{mj}}\sqrt{1-\kappa_3}\sin^2\theta_N\right) a_1'^{\dagger} \\ \left(\sqrt{1-\kappa_2} + e^{i\varphi_{mj}}\sqrt{1-\kappa_3}\right)\sin\theta_N\cos\theta_N a_1'^{\dagger} \end{pmatrix}. \end{aligned} \tag{A1}$$

Equation (A1) can also be expressed as

$$\begin{aligned} a_1'^{\dagger} \to &\left(\sqrt{1-\kappa_2}\cos^2\theta_N - e^{i\varphi_{mj}}\sqrt{1-\kappa_3}\sin^2\theta_N\right) a_1''^{\dagger} \\ &+ \left(\sqrt{1-\kappa_2} + e^{i\varphi_{mj}}\sqrt{1-\kappa_3}\right)\sin\theta_N\cos\theta_N a_r''^{\dagger} \end{aligned} \tag{A2}$$

where we have deleted the vacuum, as it has no contribution to the outputs.

All the MZIs in the inner chain can be derived the same way as in equation (A1). Consequently, the outputs of the inner chain can be obtained,

$$\begin{aligned}\begin{pmatrix} a_1'^{\dagger} \\ a_r'^{\dagger} \end{pmatrix} &= \begin{bmatrix} \cos\theta_N & -\sin\theta_N \\ \sin\theta_N & \cos\theta_N \end{bmatrix} \begin{bmatrix} \cos\theta_N & -\sin\theta_N \\ \sin\theta_N & \cos\theta_N \end{bmatrix} \\ &\times \prod_{j=1,,,N-1} \begin{bmatrix} \sqrt{1-\kappa_2}\cos\theta_N & -\sqrt{1-\kappa_2}\sin\theta_N \\ e^{i\varphi_{mj}}\sqrt{1-\kappa_3}\sin\theta_N & e^{i\varphi_{mj}}\sqrt{1-\kappa_3}\cos\theta_N \end{bmatrix} \\ &\times \begin{pmatrix} a_1'^{\dagger} \\ a_0'^{\dagger} \end{pmatrix}. \end{aligned} \tag{A3}$$

The same as (A2), the total transformation can be rewritten as

$$a_1'^{\dagger} \to M_{11}' a_1'^{\dagger} + M_{21}' a_r'^{\dagger} \tag{A4}$$

where

$$\begin{aligned} M_{11}' &= \begin{bmatrix} 1 & 0 \end{bmatrix} \begin{bmatrix} \cos\theta_N & -\sin\theta_N \\ \sin\theta_N & \cos\theta_N \end{bmatrix} \\ &\times \prod_{j=1,,,N-1} \begin{bmatrix} \sqrt{1-\kappa_2}\cos\theta_N & -\sqrt{1-\kappa_2}\sin\theta_N \\ e^{i\varphi_{mj}}\sqrt{1-\kappa_3}\sin\theta_N & e^{i\varphi_{mj}}\sqrt{1-\kappa_3}\cos\theta_N \end{bmatrix} \\ &\times \begin{bmatrix} 1 \\ 0 \end{bmatrix} \end{aligned} \tag{A5a}$$

$$\begin{aligned} M_{21}' &= \begin{bmatrix} 0 & 1 \end{bmatrix} \begin{bmatrix} \cos\theta_N & -\sin\theta_N \\ \sin\theta_N & \cos\theta_N \end{bmatrix} \\ &\times \prod_{j=1,,,N-1} \begin{bmatrix} \sqrt{1-\kappa_2}\cos\theta_N & -\sqrt{1-\kappa_2}\sin\theta_N \\ e^{i\varphi_{mj}}\sqrt{1-\kappa_3}\sin\theta_N & e^{i\varphi_{mj}}\sqrt{1-\kappa_3}\cos\theta_N \end{bmatrix} \\ &\times \begin{bmatrix} 1 \\ 0 \end{bmatrix}. \end{aligned} \tag{A5b}$$

Appendix B. The outer chain

The left output of the inner chain will go back to the outer chain. The input of the inner chain comes from the outer chain together with the vacuum. Hence, the inner chain can be regarded as the right path of the MZIs of the outer chain with dissipation $1 - M_{11}'^2$. In this way, the coefficients (M_1 and M_2) of $a_R^{\dagger}$ and $a_L^{\dagger}$ in equation (3) can be calculated from

$$\begin{aligned} M_1 &= \begin{bmatrix} 1 & 0 \end{bmatrix} \begin{bmatrix} \cos\theta_M & -\sin\theta_M \\ \sin\theta_M & \cos\theta_M \end{bmatrix} \\ &\times \prod_{k=1,2,,,M-1} \left\{ \begin{bmatrix} e^{i\phi_k}\sqrt{1-\kappa_1} & 0 \\ 0 & M'_{11} \end{bmatrix} \right. \\ &\left. \times \begin{bmatrix} \cos\theta_M & -\sin\theta_M \\ \sin\theta_M & \cos\theta_M \end{bmatrix} \right\} \begin{bmatrix} 1 \\ 0 \end{bmatrix} \end{aligned} \tag{B1a}$$

$$\begin{aligned} M_2 &= \begin{bmatrix} 0 & 1 \end{bmatrix} \begin{bmatrix} \cos\theta_M & -\sin\theta_M \\ \sin\theta_M & \cos\theta_M \end{bmatrix} \\ &\times \prod_{k=1,2,,,M-1} \left\{ \begin{bmatrix} e^{i\phi_k}\sqrt{1-\kappa_1} & 0 \\ 0 & M'_{11} \end{bmatrix} \right. \\ &\left. \times \begin{bmatrix} \cos\theta_M & -\sin\theta_M \\ \sin\theta_M & \cos\theta_M \end{bmatrix} \right\} \begin{bmatrix} 1 \\ 0 \end{bmatrix} \end{aligned} \tag{B1b}$$

where ϕ_k is the phase fluctuation of the left path in the kth outer chain, and follows the random normal distribution ($P(\phi_k) = \frac{1}{\sqrt{2\pi}\Delta_{\text{outer}}}\exp\left(-\frac{\phi_k^2}{2\Delta_{\text{outer}}^2}\right)$; Δ_{outer} is the phase fluctuation of the left path of the outer chain).

The coefficient, M_{3i}, is one of the two output fields of the ith inner chain (see figure 1(a)). Please note that M_{3i} is proportional the input field of the ith inner chain, which is one of the two output fields of the ith MZI of the outer chain, $M_{i(\text{inner})}a_r'^{\dagger}$. The output of the ith BS_M of the outer chain can be obtained with the same method as in appendix A with θ_N replaced by θ_M, and the dissipation matrix $\begin{bmatrix} \sqrt{1-\kappa_2} & 0 \\ 0 & \sqrt{1-\kappa_3} \end{bmatrix}$ replaced by $\begin{bmatrix} e^{i\phi_i}\sqrt{1-\kappa_1} & 0 \\ 0 & M'_{11} \end{bmatrix}$, so

that we have

$$M_{i\,(\mathrm{inner})} = \begin{bmatrix} 0 & 1 \end{bmatrix} \begin{bmatrix} \cos\theta_M & -\sin\theta_M \\ \sin\theta_M & \cos\theta_M \end{bmatrix} \times \prod_{k=1,2,,,i-1} \left\{ \begin{bmatrix} \mathrm{e}^{\mathrm{i}\phi_k}\sqrt{1-\kappa_1} & 0 \\ 0 & M'_{11} \end{bmatrix} \times \begin{bmatrix} \cos\theta_M & -\sin\theta_M \\ \sin\theta_M & \cos\theta_M \end{bmatrix} \right\} \begin{bmatrix} 1 \\ 0 \end{bmatrix} \tag{B2}$$

with the coefficient $M_{i\,(\mathrm{inner})}$ in hands, the coefficient of the output operator to D_{3i}, M_{3i}, can be given:

$$M_{3i} = \begin{bmatrix} 0 & 1 \end{bmatrix} \begin{bmatrix} \cos\theta_N & -\sin\theta_N \\ \sin\theta_N & \cos\theta_N \end{bmatrix} \times \prod_{j=1,,,N-1} \begin{bmatrix} \sqrt{1-\kappa_2}\cos\theta_N & -\sqrt{1-\kappa_2}\sin\theta_N \\ \mathrm{e}^{\mathrm{i}\varphi_{mj}}\sqrt{1-\kappa_3}\sin\theta_N & \mathrm{e}^{\mathrm{i}\varphi_{mj}}\sqrt{1-\kappa_3}\cos\theta_N \end{bmatrix} \times \begin{bmatrix} M_{i\,(\mathrm{inner})} \\ 0 \end{bmatrix}. \tag{B3}$$

References

[1] Bennett C H and Brassard G 1984 *Systems and Signal Processing Proc. of IEEE International Conference on Computers (Bangalore, India)* (New York: IEEE) 175

[2] Hwang W-Y, Ahn D and Hwang S W 2001 *Phys. Rev.* A **64** 064302

[3] Hwang W-Y and Matsumoto K 2002 *Phys. Rev.* A **66** 052311

[4] Hwang W-Y 2003 *Phys. Rev. Lett.* **91** 057901

[5] Rubenok A, Slater J A, Chan P, Lucio-Martinez I and Tittel W 2013 *Phys. Rev. Lett.* **111** 130501

[6] Ekert A K 1991 *Phys. Rev. Lett.* **67** 661

[7] Silberhorn Ch, Korolkova N and Leuchs G 2002 *Phys. Rev. Lett.* **88** 167902

[8] Cerf N J, Lévy M and Assche G 2001 *Van Phys. Rev. A.* **63** 052311

[9] el Allati A, el Baz M and Hassouni Y 2011 *Quantum Inf. Process* **10** 589

[10] Garcia-Patron R and Nicolas J 2009 *Cerf. Phys. Rev. Lett.* **102** 130501

[11] Jouguet P, Kunz-Jacques S and Diamanti E 2013 *Phys. Rev.* A **87** 062313

[12] Ma X-C, Sun S-H, Jiang M-S and Liang L-M 2013 *Phys. Rev.* A **88** 022339

[13] Salih H, Li Z-H, Al-Amri M and Zubairy M S 2013 *Phys. Rev. Lett.* **110** 170502

[14] Kwiat P, Weinfurter H, Herzog T, Zeilinger A and Kasevich A 1995 *Phys. Rev. Lett.* **74** 4763

[15] Karlsson A, Bjrk G and Forsberg E 1998 *Phys. Rev. Lett.* **80** 1198

[16] Tsegaye T, Goobar E, Karlsson A, Bjrk G, Loh M Y and Li K H 1998 *Phys. Rev.* A **57** 3987

[17] Kwiat P G, White A G, Mitchell J R, Nairz O, Weihs G, Weinfurter H and Zeilinger A 1999 *Phys. Rev. Lett.* **83** 4725

[18] Lim C C W, Curty M, Walenta N, Xu F and Zbinde H 2014 *Phys. Rev.* A **89** 022307

[19] Meyer-Scott E, Yan Z, MacDonald A, Bourgoin J-P, Hubel H and Jennewein T 2011 *Phys. Rev.* A **84** 062326

[20] Curty M and Morod T 2007 *Phys. Rev.* A **75** 052336